

## Scattering Investigation of Acoustic Localization in Fused Silica

Marie Foret,<sup>1</sup> Eric Courtens,<sup>1</sup> René Vacher,<sup>1</sup> and Jens-Boie Suck<sup>2</sup>

<sup>1</sup>Laboratoire des Verres,\* Université de Montpellier II, F-34095 Montpellier, France

<sup>2</sup>Institut für Physik, T.U. Chemnitz-Zwickau, D-09107 Chemnitz, Germany

(Received 28 May 1996)

Small angle neutron time-of-flight spectroscopy and inelastic x-ray scattering results are reported on the acoustic vibrations of fused silica. An expression for the dynamical structure factor is given that successfully describes the scattering from these vibrations, including the boson peak. The data analysis indicates an acoustic localization edge at  $\cong 1$  THz, in agreement with the position of the thermal conductivity plateau. Scattering results on another strong glass support the generality of our description. [S0031-9007(96)01538-4]

PACS numbers: 63.50.+x, 61.10.-i, 61.12.-q

The nature of vibrational excitations in glasses remains a question of considerable current interest [1]. In these materials, acoustic waves propagate up to relatively high frequencies  $\omega$ , in spite of the structural disorder. For example, in vitreous silica,  $v$ -SiO<sub>2</sub>, the velocities  $c$  of acoustic waves, both longitudinal (LA) and transverse (TA), do not show appreciable deviations from a linear dispersion up to the highest measured  $\omega \approx 400$  GHz [2]. The linewidth  $\Gamma$  of these waves is found to be proportional to  $\omega^2$  over the accessible  $\omega$  range [3,4]. However, owing to the disorder, one expects that Rayleigh scattering of acoustic waves, leading to  $\Gamma \propto \omega^4$  for *plane* waves, should eventually take over at sufficiently high  $\omega$  [5,6]. This should then rapidly lead to the Ioffe-Regel (IR) regime [7], in which  $\Gamma = \omega$  for  $\omega > \omega_{\text{IR}}$ , where  $\omega_{\text{IR}}$  is the IR-crossover frequency. In this strong phonon-scattering limit the vibrational eigenmodes must be controlled by a single length scale, which plays simultaneously the role of a wavelength, a scattering length, and a localization length [8]. This view agrees with the existence of a thermal conductivity plateau at low temperatures  $T \approx 10$  K [9], indicating that acoustic excitations must cease to propagate when their wavelength  $\lambda$  reaches the nm range [10–12]. There exists, however, no direct measurement of the crossover at  $\omega_{\text{IR}}$ . In this Letter, we combine for the first time the results of neutron and x-ray Brillouin-scattering spectroscopies to pin down the value of  $\omega_{\text{IR}}$  in  $v$ -SiO<sub>2</sub>. Moreover, in this system a relatively large boson peak is observed [13]. The origin of this universal feature in glasses is still strongly debated. From our analysis we obtain compelling evidence that the boson peak is simply the scattering from localized acoustic excitations.

The linewidths  $\Gamma$  of  $v$ -SiO<sub>2</sub> at room temperature are illustrated in Fig. 1. The large  $\omega$  region with  $\Gamma \propto \omega^2$  suggests very fast relaxation, or anharmonic interactions [3,4]. The Rayleigh law predicted from thermal conductivity [6] is shown by the dashed line, up to the IR limit. In this Letter we show that the IR crossover is indeed found at  $\omega_{\text{IR}}/2\pi \cong 1$  THz, i.e., strikingly close to the prediction (Fig. 1). The corresponding wavelength appears to be rather large,  $2\pi c_0/\omega_{\text{IR}} \cong 6$  nm, where

the LA velocity  $c_0 = 5900$  m/s is used. This, however, gives a crossover wave vector  $q_{\text{IR}} \cong 1.0$  nm<sup>-1</sup>, in remarkable agreement with early estimates [10].

Two new techniques have recently been developed at large facilities which allow Brillouin-scattering experiments with frequency shifts  $\omega$  in the THz range [14,15]. The first is the neutron Brillouin-scattering option on the cold-neutron spectrometer IN5 at the Institut Laue-Langevin (ILL) in Grenoble, France. It combines a large position-sensitive detector (PSD) at small angles with high resolution time-of-flight spectroscopy. Wave vectors  $q$  in the nm<sup>-1</sup> range can be reached with energy resolutions well below 1 meV. However, for *propagating* modes with *linear* dispersion, the simultaneous conservation of energy and momentum (kinematic conditions) requires incident neutrons of velocity at least equal to  $\sim 1.2$  to 1.4 times the phase velocity under investigation [14].

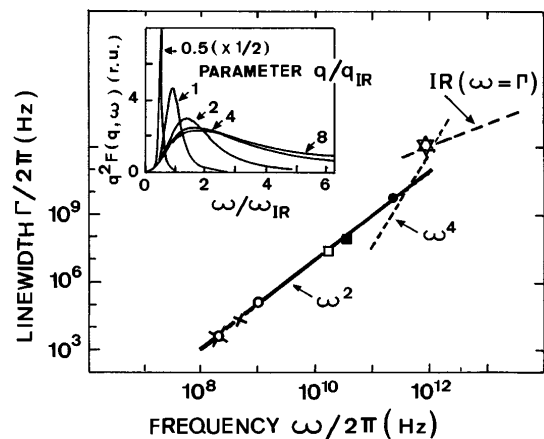


FIG. 1. The linewidth  $\Gamma$  of acoustic phonons in  $v$ -SiO<sub>2</sub>, from ultrasonic [LA(○), TA(x)], Brillouin [LA(■), TA(□)], and picosecond optics (●) measurements as room temperature [3,4]. A line  $\Gamma \propto \omega^2$  is traced through the points. The dashed lines are quantitative predictions using the strength of phonon Rayleigh scattering from Ref. [6]. The Ioffe-Regel limit found in this study is  $\star$ . The inset illustrates the spectral function  $q^2 F(q, \omega)$  at a few values of  $q/q_{\text{IR}}$  for parameters adequate to  $v$ -SiO<sub>2</sub>.

High  $\omega$  resolution being obtained with slow neutrons, the kinematic conditions can only be fulfilled for phase velocities well below the speed of sound of strong glasses. Hence, a second instrument is of particular interest. It is the inelastic x-ray spectrometer ID16 at the European Synchrotron Radiation Facility (ESRF) in Grenoble, that became operational last year. Most recently, resolutions of 2 meV and 1 nm<sup>-1</sup> were achieved [15]. Owing to the high energy of x-rays, the kinematic conditions are always satisfied. The main difficulty here is the low intensity of the inelastic scattering from strong glasses, which overlaps the wings of an intense elastic scattering. This restricts such experiments to samples with sufficiently small composition fluctuations, e.g., *v*-SiO<sub>2</sub>.

On IN5 we used an incident neutron wavelength of 2.5 Å. The resolution obtained from the width of the elastic peak of a vanadium calibration spectra was 1.0 meV (242 GHz) (FWHM). The two-dimensional PSD was grouped into 15 concentric rings of 2 cm width each, covering *elastic*  $q$  values from 0.7 to 3.4 nm<sup>-1</sup>. Besides the PSD, IN5 was covered with 90 detectors up to a scattering angle of 130°. The sample, measured at room  $T$ , was a 0.75 cm thick slab of Suprasil. It was placed between Cd sheets forming a 5 × 2.5 cm<sup>2</sup> window. After subtraction of the empty can run and absorption corrections, the remaining intensity was converted into the dynamic structure factor  $S(q, \omega)$  using the  $V$ -calibration run measured under identical experimental conditions. In Fig. 2, four sections through  $S(q, \omega)$  are shown. Owing to the kinematic constraints, the accessible  $\omega$  region decreases together with  $q$ .

The data exhibit a  $q$ -dependent broad peak with a maximum about 4 meV. This value is remarkably close to the anticipated  $\omega_{\text{IR}}$  (Fig. 1). It also corresponds to a

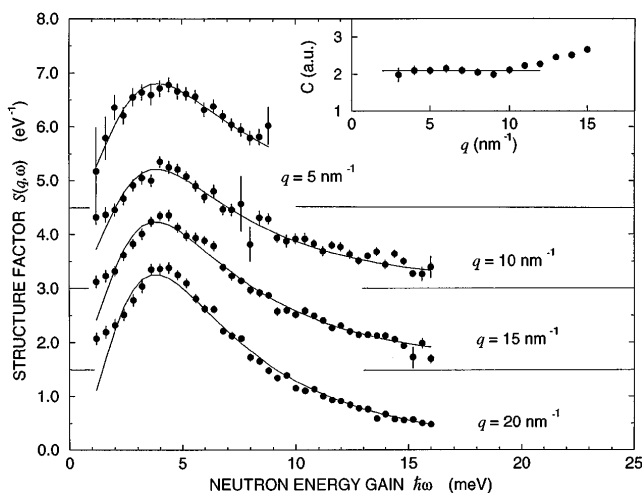


FIG. 2. Constant- $q$  sections through  $S(q, \omega)$  on the neutron-energy gain side (anti-stokes) in *v*-SiO<sub>2</sub>. The base lines are shifted vertically as shown. The fits are obtained with a single  $\omega_{\text{IR}}$  and the prefactors  $C$  [Eq. (4)] as free parameters. The inset illustrates the near constancy of  $C$  derived from the fits.

crossover in the density of states,  $N(\omega)$ , derived from specific heat data as shown in Fig. 1 of Ref. [16]. It is reminiscent of the corresponding situation in silica aerogels, where light scattering revealed a crossover between LA phonons and localized states [17]. The strongly *inhomogeneously* broadened light-scattering spectra of aerogels in the crossover region were exactly described by a spectral function  $F(q, \omega)$  derived from a Green function analysis [18], complemented by empirical considerations [17]. Although originally applied to a percolation model [18], that expression remains valid for systems that are *not* fractal at  $q > q_{\text{IR}}$ . All that is required is a clear onset of strong phonon scattering. The physical picture is that, as  $\omega$  increases towards  $\omega_{\text{IR}}$ , the definition in  $q$  of the vibrations becomes less and less precise. Thus vibrations of different frequencies have an appreciable Fourier component at the scattering vector  $q$ . This leads to a dependence in frequency (rather than in  $q$ , which is not well defined *for the vibrations*) of the parameters entering  $F(q, \omega)$ . These are the linewidth,  $\Gamma(\omega)$ , and the velocity,  $c(\omega)$ , which beyond  $\omega_{\text{IR}}$  really accounts for the density of states. The equations of Ref. [17] are rewritten as

$$F(q, \omega) = \frac{c^2 q^2}{\omega} \frac{\Gamma}{(\omega^2 + \Gamma^2 - c^2 q^2)^2 + 4\Gamma^2 c^2 q^2}, \quad (1)$$

$$\Gamma(\omega) = \frac{\omega^4}{\omega_{\text{IR}}^3} [1 + (\omega/\omega_{\text{IR}})^m]^{-3/m}, \quad (2)$$

$$c(\omega) = c_0 [1 + (\omega/\omega_{\text{IR}})^m]^{\zeta/m}. \quad (3)$$

A multiplicative constant is left out of (1). The IR crossover is included in (2) and (3). The exponent  $m$  describes the sharpness of the IR crossover. The velocity  $c(\omega)$  takes the known value  $c_0$  at low  $\omega$ , and it is  $\propto \omega^\zeta$  at high  $\omega$ . The exponent  $\zeta$  reflects the  $\omega$  dependence of  $N(\omega) \propto \omega^{d-1-d\zeta}$ . Here,  $d = 3$  is the space dimensionality, appropriate to the mass distribution at this scale. The experimental  $N(\omega)$  of *v*-SiO<sub>2</sub> shows a region in  $\sim \omega^{0.9}$ , from  $\omega_{\text{IR}}$  to 10 meV [16]. This gives  $\zeta = 0.37$ .

The large amount of data [17] fitted with this  $F(q, \omega)$  validates its  $q$  and  $\omega$  dependence, up to a prefactor in  $q$  not accessible to light-scattering spectroscopy, but which could now be determined in neutron scattering. For direct coupling to one-phonon scattering, one has [14]

$$S(q, \omega) = C n_B e^{-2W} q^2 F(q, \omega), \quad (4)$$

where  $C$  includes all multiplicative constants,  $n_B$  is the Bose-Einstein factor, and  $e^{-2W}$  is the Debye-Waller factor. The one-phonon  $S(q, \omega)$  is the dominant contribution at the low  $q$  values of this experiment, while  $e^{-2W}$  can be approximated by 1 for these  $q$  values in *v*-SiO<sub>2</sub> at room  $T$ . The inset of Fig. 1 illustrates  $q^2 F(q, \omega)$  for typical values of  $q/q_{\text{IR}}$ . After further multiplication by  $n_B$ , it is easy to see that the integral of the Brillouin peak in the phonon regime ( $c_0 q < \omega_{\text{IR}}$ ) is constant. One notes that

for  $q \gg q_{\text{IR}}$ , the profile becomes practically  $q$  independent, with a peak slightly above  $\omega_{\text{IR}}$ .

Constant- $q$  sections of the data were fitted with Eqs. (1)–(4) convoluted with the instrumental function as shown in Fig. 2. The range actually used for the fits is from 2 to 10 meV. Below 2 meV, the *relaxational* contribution, not included in (1), becomes important [19]. One knows [8,18] that Eqs. (1)–(3), although an excellent crossover expression, are not designed to describe scattering at  $\omega \gg \omega_{\text{IR}}$ , or at  $q \gg q_{\text{IR}}$ . However, we remark that the agreement between the data and the calculated lines persists well above 10 meV [20]. It also extends to fairly large  $q$ . Leaving  $m$  as a free parameter, it takes a value very close to 2. It was then fixed at 2 for the fits shown here. Allowing for different intensity prefactors  $C$  for each  $q$ , one finds that  $C$  increases slightly at the largest  $q$  values. It is, however, remarkably constant up to  $q/q_{\text{IR}}$  as large as 10, as shown in the inset of Fig. 2. This gives great confidence in the expression for  $S(q, \omega)$ . From  $\omega_{\text{IR}} = 3.9 \pm 0.1$  meV, and the velocity  $c_0$  of the LA phonon, one finds  $q_{\text{IR}} = 1.0 \text{ nm}^{-1}$ . The experimental point shown on the IR limit in Fig. 1 corresponds to this  $\omega_{\text{IR}}$ .

To achieve smaller  $q$  values, an inelastic x-ray scattering experiment at 17.8 KeV was performed on ID16 at the ESRF. The experimental setup is described extensively elsewhere [15]. The sample consisted of an optically polished Suprasil slab of 3 mm thickness. The scattering is observed at small angles in transmission. The instrumental function was obtained from the scattering of the sample cooled to 20 K. At that low  $T$ , practically all the scattering is elastic. We find an energy resolution of 3.2 meV FWHM. The entire data in Fig. 3 were accumulated at room  $T$  for a total counting time of  $\sim 40$  h. The  $q$  resolution limited by the finite acceptance angle, is  $\sim 0.3 \text{ nm}^{-1}$  at  $q = 1.5$  and  $2 \text{ nm}^{-1}$ , and  $\sim 0.5 \text{ nm}^{-1}$  at  $3$  and  $4 \text{ nm}^{-1}$ . An empty cell measurement at the smallest scattering angle revealed a flat electronic background plus elastic scattering from the cell windows. A background of 1.9 counts/mn, in agreement with the experimental determination, is subtracted from the data shown in Fig. 3. A typical spectrum is shown enlarged in Fig. 3(a). The data in the wings are clearly above the elastic instrumental function. In Fig. 3(b), the fitted elastic peaks have been subtracted, the errors bars being increased accordingly. Fits to the entire data were performed with  $S(q, \omega)$  from Eq. (4). At this resolution, the relaxational part is essentially contained within the elastic peak. The solid lines in Fig. 3(b) result from fixing all parameters to the values found in neutron scattering, taking the  $q$  resolution into account, and convoluting with the instrumental function. The only free parameters are the intensities. The  $\chi^2$  is better than 0.5. To within the uncertainty margins related to the weakness of the signals and the size of the collection angles, we find that  $C$  in Eq. (4) is independent of  $q$ . If, additionally,  $\omega_{\text{IR}}$  is left free in a

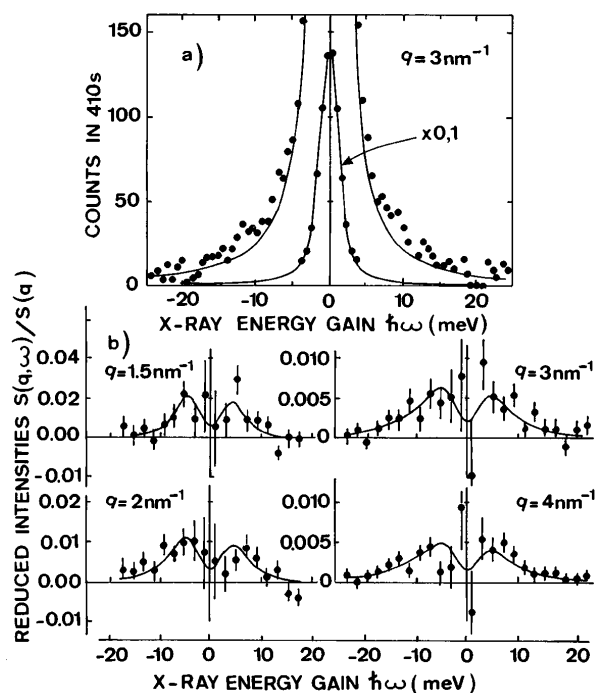


FIG. 3. (a) Inelastic x-ray scattering spectrum at  $q = 3 \text{ nm}^{-1}$  after background subtraction (points) compared to the instrumental profile measured on the sample at 20 K (line). The intensity of the line is adjusted to match the elastic peak of the data as shown on a reduced scale in the center. (b) The inelastic part of the spectra after subtraction of the elastic peaks. Compared to (a), the points here are grouped 3 by 3 in view of the weak signals. The lines are fits to Eq. (4) with the intensities as only free parameters.

joint fit of all four x-ray spectra, one recovers the  $\omega_{\text{IR}}$  of the neutron data within a confidence interval of about  $\pm 1.5$  meV. In spite of the weak signals, two important conclusions can be drawn: There is only one fairly broad peak, that broadens with increasing  $q$ , and there are no propagating phonons following a linear dispersion which, at  $q = 4 \text{ nm}^{-1}$ , would correspond to  $\omega = 15$  meV.

In conclusion, spectroscopic evidence indicates that LA excitations, which propagate for  $q = 0.7 \text{ nm}^{-1}$  [2], are already localized at  $q = 1.5 \text{ nm}^{-1}$ . For  $q > q_{\text{IR}}$ , there is *no kinematic condition* to fulfill on  $q$ . Hence, the boson peak seen in neutron scattering is simply scattering from these localized vibrations. This appears different from recent results on fragile glasses in which an acoustic mode was claimed to propagate at  $\omega$  above the boson peak [15]. Our analysis provides a successful expression to fit scattering from localized vibrations in a  $(q, \omega)$  region around  $\omega_{\text{IR}}$  and  $q_{\text{IR}}$ . It is particularly useful when  $N(\omega)$  is known [20]. In that case, only three parameters, namely,  $\omega_{\text{IR}}$ ,  $C$ , and  $m$ , need to be adjusted to fit  $S(q, \omega)$  up to large  $\omega/\omega_{\text{IR}}$  and  $q/q_{\text{IR}}$ . When localized, the vibrations are expected to lose their pure longitudinal or transverse character, but, for direct coupling to density fluctuations [21], neutrons, or x-rays, continue to probe

the longitudinal projection of the vibrations. Conversely, Raman scattering takes place in the very long wave limit,  $q \ll q_{\text{IR}}$ . The direct coupling is then very weak in comparison to other mechanisms, such as the acousto-optic (Pockels) or the dipole-induced dipole ones [21]. This introduces other  $\omega$  dependences in the spectrum (leading to the Raman coupling coefficient), as well as contributions from transverse vibrational components. The above views on the boson peak are vindicated by recent computer simulations on a strong glass [22]. The latter clearly show that, as  $q$  is increased, the acoustic mode localizes at fairly low  $q$  while the spectrum strongly changes shape around  $q_{\text{IR}}$ . It is intuitive that the numerical results presented in Fig. 8 of Ref. [22] could be described very well by line shapes such as those in the inset of our Fig. 1. It should be remarked that no particular “hump” in the density of states is needed to explain the boson peak.

Results similar to those of Fig. 2 were obtained on a heavy flint containing  $\text{SiO}_2$ ,  $\text{PbO}$ , and  $\text{BaO}$  with  $\approx 30$ , 49, and 17 wt. %, respectively. In this case, the smaller value of  $c_0$  (3800 m/s) brings one closer to the kinematic conditions, producing a slightly stronger  $q$  dependence at small  $q$  values. One obtains excellent fits with Eqs. (1)–(4), with  $\omega_{\text{IR}} = 3.2 \pm 0.1$  meV, which gives  $q_{\text{IR}} = 1.3 \text{ nm}^{-1}$ . This confirms that a mixed glass is somewhat more homogeneous than  $\nu\text{-SiO}_2$  at the medium-range scale [5]. More importantly, it indicates that our approach extends beyond the single example of  $\nu\text{-SiO}_2$ .

This work benefited from the advice of F. Sette and the generous help of his team, in particular, C. Masciovecchio, M. Krisch, and R. Verbeni. Thanks are also expressed to J. Pelous for stimulating discussions, to K. Andersen for assistance on IN5, to S. Alexander for critical comments on the manuscript, to H. Arribart at Saint-Gobain for the heavy flint, to G. Ruocco and M. Soltwisch for discussions and for a preprint of Ref. [15], and to B. Delettre for expert polishing.

\*UMR No. 5587 of the Centre National de la Recherche Scientifique (CNRS).

- [1] See, e.g., the Proceedings of the *Combined Conference of the 4th International Conference on Phonon Physics and the 8th International Conference on Phonon Scattering in Condensed Matter*. *Phonons 95* [Physica (Amsterdam) **219B-220B**, (1996)].
- [2] M. Rothenfusser, W. Dietsche, and H. Kinder, in *Phonon Scattering in Condensed Matter*, edited by W. Eisenmenger, K. Lassmann, and S. Döttinger (Springer, Berlin, 1984), p. 419.
- [3] R. Vacher, J. Pelous, F. Plicque, and A. Zarembowitch, *J. Non-Cryst. Solids* **45**, 397 (1981).

- [4] C.-D. Zhu, H. J. Maris, and J. Tauc, in *Phonons 89*, edited by S. Hunklinger, W. Ludwig, and G. Weiss (World Scientific, Singapore, 1990), p. 498; C. J. Marath, G. Tas, T. C.-D. Zhu, and H. J. Maris, *Physica (Amsterdam)* **219B-220B**, 296 (1996).
- [5] S. R. Elliot, *Europhys. Lett.* **19**, 201 (1992).
- [6] J. Jäckle, in *Proceedings of the IVth International Conference on the Physics of Non-Crystalline Solids*, edited by G. H. Frischat, (Trans. Tech., Ädermannsdorf, 1977), p. 568.
- [7] A. F. Ioffe and A. R. Regel, *Prog. Semicond.* **4**, 237 (1960).
- [8] S. Alexander, *Phys. Rev. B* **40**, 7953 (1989).
- [9] R. C. Zeller and R. O. Pohl, *Phys. Rev. B* **4**, 2029 (1971).
- [10] C. Kittel, *Phys. Rev.* **75**, 972 (1949).
- [11] S. Alexander, C. Laermans, R. Orbach, and H. M. Rosenberg, *Phys. Rev. B* **28**, 4615 (1983).
- [12] J. E. Graebner, B. Golding, and L. C. Allen, *Phys. Rev. B* **34**, 5696 (1986); J. E. Graebner and B. Golding, *Phys. Rev. B* **34**, 5788 (1986).
- [13] E.g., A. P. Sokolov, A. Kisliuk, D. Quitmann, A. Kudlik, and E. Rössler, *J. Non-Cryst. Solids* **172-174**, 138 (1994).
- [14] P. A. Egelstaff, G. Kearley, J.-B. Suck, and J. P. A. Youden, *Europhys. Lett.* **10**, 37 (1989); J.-B. Suck, P. A. Egelstaff, R. A. Robinson, D. S. Sivia, and A. D. Taylor, *Europhys. Lett.* **19**, 207 (1992).
- [15] C. Masciovecchio, G. Ruocco, F. Sette, M. Krisch, R. Verbeni, U. Bergman, and M. Soltwisch, *Phys. Rev. Lett.* **76**, 3356 (1996).
- [16] U. Buchenau, M. Prager, N. Nücker, A. J. Dianoux, N. Ahmad, and W. A. Phillips, *Phys. Rev. B* **34**, 5665 (1986).
- [17] E. Courtens, R. Vacher, J. Pelous, and T. Woignier, *Europhys. Lett.* **6**, 245 (1988); E. Anglaret, A. Hasmy, E. Courtens, J. Pelous, and R. Vacher, *Europhys. Lett.* **28**, 591 (1994).
- [18] G. Polatsek and O. Entin-Wohlman, *Phys. Rev. B* **37**, 7726 (1988).
- [19] A. P. Sokolov, U. Buchenau, W. Steffen, B. Frick, and A. Wischnewski, *Phys. Rev. B* **52**, R9815 (1995).
- [20] To obtain this excellent agreement, a further feature of the experimental density of states, i.e.,  $N(\omega) \propto \omega^0$  for  $\omega > 10 \text{ meV}^{16}$ , was included in  $c(\omega)$  [Eq. (3)] in the form of a second multiplicative crossover. For the latter, one finds the exponent  $z' = 0.3$  from  $d - 1 - (z + z')d = 0$ . This additional crossover at 10 meV does not change  $S(q, \omega)$  in the region where fits are made ( $\omega < 10 \text{ meV}$ ). However, it provides a remarkable agreement between the calculation and the data points also above 10 meV (Fig. 2).
- [21] S. Alexander, E. Courtens, and R. Vacher, *Physica (Amsterdam)* **195A**, 286 (1993).
- [22] R. Fernández-Perea, F. J. Bermejo, and E. Enciso, *Phys. Rev. B* **53**, 6215 (1996).